

VINP: Variational Bayesian Inference with Neural Speech Prior for Joint ASR-Effective Speech Dereverberation and Blind RIR Identification

Pengyu Wang[✉], Ying Fang[✉], and Xiaofei Li[✉]

Abstract—Reverberant speech, denoting the speech signal degraded by the process of reverberation, contains crucial knowledge of both anechoic source speech and room impulse response (RIR). This work proposes a variational Bayesian inference (VBI) framework with neural speech prior (VINP) for joint speech dereverberation and blind RIR identification. In VINP, a probabilistic signal model is constructed in the time-frequency (T-F) domain based on convolution transfer function (CTF) approximation. For the first time, we propose using an arbitrary discriminative dereverberation deep neural network (DNN) to predict the prior distribution of anechoic speech within a probabilistic model. By integrating both reverberant speech and the anechoic speech prior, VINP yields the maximum a posteriori (MAP) and maximum likelihood (ML) estimations of the anechoic speech spectrum and CTF filter, respectively. After simple transformations, the waveforms of anechoic speech and RIR are estimated. Moreover, VINP is effective for automatic speech recognition (ASR) systems, which sets it apart from most deep learning (DL)-based single-channel dereverberation approaches. Experiments on single-channel speech dereverberation demonstrate that VINP reaches an advanced level in most metrics related to human perception and displays unquestionable state-of-the-art (SOTA) performance in ASR-related metrics. For blind RIR identification, experiments indicate that VINP attains the SOTA level in blind estimation of reverberation time at 60 dB (RT60) and direct-to-reverberation ratio (DRR). Codes and audio samples are available online¹.

Index Terms—Speech dereverberation, reverberation impulse response identification, variational Bayesian inference, convolutional transfer function approximation, deep learning.

I. INTRODUCTION

REVERBERATION, which is formed by the superposition of multiple reflections, scattering, and attenuation of sound waves in a closed space, is one of the main factors degrading speech quality and intelligibility in daily life. The reverberant speech contains the crucial knowledge of both anechoic source speech and room impulse response (RIR). The anechoic speech, often regarded as an oracle, serves as the ultimate target of speech dereverberation. Moreover, RIR characterizes the sound propagation from sound source to microphone constrained in a room environment. Therefore,

given a reverberant microphone recording, there is a strong need to estimate the anechoic speech and RIR, leading to two distinct tasks: speech dereverberation and blind RIR identification, respectively.

A series of classical speech dereverberation approaches build deterministic signal models of anechoic source speech, RIR, and reverberant microphone recording. After that, dereverberation is solved by designing an inverse filter in the time domain [1] or time-frequency (T-F) domain [1], [2], [3], [4], [5]. In contrast, another series of classical methods regard the anechoic source speech signal and the reverberant microphone recording as random variables, and use hierarchical probabilistic graphical models to describe the conditional independent relationship between these random variables. Speech dereverberation is then performed by estimating every unknown latent variable and model parameter, including the anechoic speech spectral coefficient and the reverberation model parameters [6], [7]. Actually, the construction of the probabilistic graphical model is highly flexible. By modeling different factors that affect the observed signal as latent variables and model parameters, similar methods can be applied to a variety of fields, such as speech denoising [6], [8], [9] and direct-of-arrival estimation [10], [11], [12]. Classical methods are model-based and unsupervised, which makes them free from generalization problems. However, due to the insufficient utilization of prior knowledge regarding speech and distortion, the performance of these methods remains unsatisfactory.

In recent decades, data-driven deep learning (DL)-based approaches have developed rapidly and surpassed the performance of classical ones. These approaches rely less on the assumptions of signal models, instead directly learn the characteristics of speech signals using deep neural networks (DNNs). Regarding such methods, the focal point of algorithm development is the design of DNN structures, network inputs and outputs, and loss functions. The most straightforward DL-based idea is to construct a discriminative DNN to learn the mapping from degraded speech to target speech. For instance, authors in [13], [14], [15], [16], [17], [18] developed various discriminative DNNs and loss functions to build mappings in various representation domains. Another concept is to consider speech dereverberation as a generative task and utilize generative DNNs, such as variational autoencoder (VAE) [19], generative adversarial network (GAN) [20], and diffusion model (DM) [21], to generate audio samples [22], [23], [24], [25]. Thanks to the powerful non-linear modeling ability of DNNs, DL-based methods are able to make the best of a

Pengyu Wang is with Zhejiang University and also with Westlake University, Hangzhou, China (e-mail: wangpengyu@westlake.edu.cn).

Ying Fang is with Zhejiang University and also with Westlake University, Hangzhou, China (e-mail: fangying@westlake.edu.cn).

Xiaofei Li is with the School of Engineering, Westlake University, and the Institute of Advanced Technology, Westlake Institute for Advanced Study, Hangzhou, China (e-mail: lixiaofei@westlake.edu.cn).

Xiaofei Li: corresponding author.

¹<https://github.com/Audio-WestlakeU/VINP>

large amount of data and typically lead to a better performance than classical ones. However, it is still challenging to improve automatic speech recognition (ASR) performance because such a single-channel front-end system without joint training always introduces artifact errors into speech waveforms [26], [27].

Particularly, some methods combine the VAE and classical methods based on probabilistic graphical models, forming a so-called semi-supervised [28], [29] or unsupervised [30], [31] branch. Unlike the supervised DL-based approaches, the VAE in these methods is trained with only clean speech utterances. At the inference stage, the VAE decoder participates in solving the probabilistic graphical model through the estimation of clean speech prior. Usually, the Markov chain Monte Carlo (MCMC) algorithm is used to sample the latent variables in VAE. Compared with classical methods, the prior generated by VAE has higher quality and can yield better speech enhancement results. Such algorithms were first applied to speech denoising [28], [29], [30] and then expanded to speech dereverberation [31], [32]. For instance, in [31], the authors developed a Monte Carlo expectation-maximization (EM) algorithm based on a convolutional VAE and non-negative matrix factorization (NMF) model. In our previous work RVAE-EM [32], we employed a more powerful recurrent VAE to learn the prior distribution of anechoic speech. Also, we found that when the anechoic speech prior is of sufficient quality, MCMC is unnecessary, thus avoiding the repeated inference by VAE decoders. Moreover, by introducing supervised data into the training of VAE, we also obtained a supervised version of RVAE-EM that performs better than the unsupervised one. This finding inspired our current work. Since there are already many advanced dereverberation DNN architectures, it is possible to directly apply them as supervised anechoic speech prior estimators to the solution of the probabilistic graphical model with some simple modifications.

Within the domain of audio signal processing, blind RIR identification from reverberant microphone recording constitutes a crucial and challenging area of research, since RIR characterizes the acoustic characteristics of the sound propagation and environment. Currently, methods for blind RIR identification are rather scarce. In recent years, with the development of DL techniques, some DL-based approaches have been proposed [33], [34], [35]. For instance, the authors in [35] established a parameterized model for the reverberation effect and proposed an unsupervised method for joint speech dereverberation and blind RIR estimation. This approach is similar to our work in terms of tasks.

In this paper, we propose a variational Bayesian inference framework with neural speech prior (VINP) for joint speech dereverberation and blind RIR identification. Our motivation is as follows: Given that the convolution transfer function (CTF) approximation is a rather accurate model of the reverberation effect, by making reasonable probabilistic assumptions and regarding the output of DNN as the prior distribution of anechoic speech, we are able to analytically estimate the anechoic spectrum and the CTF filter, and further obtain the time-domain waveforms of anechoic speech and RIR. The basis of VINP is a probabilistic signal model based on CTF

approximation [36], the same as in our previous work RVAE-EM [32]. The signal model describes the relationship among the source speech, CTF filter, and reverberant microphone recording. Different from RVAE-EM [32], considering the existence of advanced discriminative DNN structures for dereverberation, we proposed to employ such DNNs to learn the prior distribution of anechoic speech by modifying the loss function of network training. Sequentially, we use variational Bayesian inference (VBI) [37], [38] to analytically solve the hidden variables and parameters in our probabilistic model. By doing this, VINP avoids the direct utilization of DNN output but still utilizes the powerful nonlinear modeling capability of the network, thereby benefiting ASR. Moreover, a major drawback of RVAE-EM [32] is that the computational cost grows with the cube of the speech length. Through the variational inference, the computational cost in the proposed method increases linearly with the speech length. Additionally, parallel computation can be used across T-F bins for fast implementation.

This paper has the following contributions:

- We propose VINP, a novel VBI framework with neural speech prior for joint speech dereverberation and blind RIR identification. For the first time, we propose introducing an arbitrary discriminative dereverberation DNN into VBI to successfully complete the tasks.
- VINP avoids the direct utilization of DNN output but still utilizes the powerful nonlinear modeling capability of the network. Thus, it can enhance the ASR performance of the original backbone DNN without the need for any joint training with the ASR system. Experiments demonstrate that VINP attains an advanced level in most metrics related to human perception and displays unquestionable state-of-the-art (SOTA) performance in ASR-related metrics.
- VINP can be used for blind RIR identification from reverberant microphone recording. Experiments indicate that VINP attains the SOTA level in the blind estimation of reverberation time at 60dB (RT60) and direct-to-reverberation ratio (DRR).
- From the perspective of computational cost, VINP exhibits linear growth with respect to the speech length, which is different from the cubical growth in our previous work RVAE-EM [32]. Moreover, the VBI procedure in VINP can be implemented in parallel across T-F bins, thereby further reducing the processing time.

The remainder of this paper is organized as follows: Section II formulates the signal model and the tasks. Section III elaborates on the proposed VINP framework. Experiments and discussions are presented in Section IV. Finally, Section V concludes the entire paper.

II. SIGNAL MODEL AND TASK DESCRIPTION

In this section, we will introduce the signal model and define two tasks we aim to address: speech dereverberation and blind RIR identification.

A. Signal Model

Considering the scenario of a single static speaker and stationary noise, the reverberant speech signal (observation) received by a distant microphone can be modeled in the time domain as

$$x(n) = h(n) * s(n) + w(n), \quad (1)$$

where $*$ is the convolution operator, n is the index of sampling points, $x(n)$ is the observation signal, $s(n)$ is the anechoic source speech signal, $h(n)$ is the RIR which describes a time-invariant linear filter, and $w(n)$ is the background additive noise. Without loss of generality, we assume that the RIR begins with the impulse response of the direct-path propagation, followed with reflections and reverberation.

Analyzing and processing speech signals in the time domain poses significant challenges. After performing short-time Fourier transform (STFT), according to the CTF approximation [36], the observation model in the T-F domain becomes

$$\begin{aligned} X(f, t) &\approx \sum_{l=0}^{L-1} H_l(f) S(f, t-l) + W(f, t) \\ &= \mathbf{H}(f) \mathbf{S}(f, t) + W(f, t), \end{aligned} \quad (2)$$

where f and t are the indices of frequency band and STFT frame, respectively; L is the length of CTF filter; $X(f, t)$, $S(f, t)$, $W(f, t)$, and $H_l(f)$ are the complex-valued observation signal, source speech signal, noise signal, and CTF coefficient, respectively; $\mathbf{H}(f) = [H_{L-1}(f), \dots, H_0(f)] \in \mathbb{C}^{1 \times L}$, $\mathbf{S}(f, t) = [S(f, t-L+1), \dots, S(f, t)]^T \in \mathbb{C}^{L \times 1}$.

Furthermore, the observation $X(f, t)$, anechoic source $S(f, t)$, and noise $W(f, t)$ are modeled as random signals. We have the following assumptions regarding their distributions.

- Assumption 1: The anechoic source speech signal $S(f, t)$ follows a time-variant zero-mean complex-valued Gaussian distribution, while the noise signal $W(f, t)$ follows a time-invariant zero-mean complex-valued Gaussian distribution. Therefore, we have their prior distributions as

$$\begin{cases} S(f, t) \sim \mathcal{CN}(0, \alpha^{-1}(f, t)) \\ W(f, t) \sim \mathcal{CN}(0, \delta^{-1}(f)), \end{cases} \quad (3)$$

where $\alpha(f, t)$ and $\delta(f)$ are the precisions of the Gaussian distributions.

- Assumption 2: The anechoic source speech signal $S(f, t)$ and noise signal $W(f, t)$ are respectively independent for all T-F bins. Defining $\mathbf{S} = [S(1, 1), \dots, S(1, T), \dots, S(F, T)]^T \in \mathbb{C}^{1 \times FT}$ and $\mathbf{W} = [W(1, 1), \dots, W(1, T), \dots, W(F, T)]^T \in \mathbb{C}^{1 \times FT}$, we have

$$\begin{cases} \mathbf{S} \sim \prod_{f=1}^F \prod_{t=1}^T p(S(f, t)) \\ \mathbf{W} \sim \prod_{f=1}^F \prod_{t=1}^T p(W(f, t)). \end{cases} \quad (4)$$

- Assumption 3: The anechoic source speech signal \mathbf{S} and noise signal \mathbf{W} are independent of each other, which means

$$\mathbf{S}, \mathbf{W} \sim p(\mathbf{S})p(\mathbf{W}). \quad (5)$$

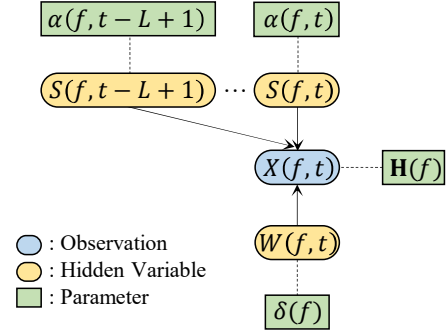


Fig. 1: Probabilistic graphical generation model of reverberant microphone recording (observation).

With all the aforementioned assumptions, the conditional probability of the observation signal can be expressed as follows.

$$\begin{cases} X(f, t) | \mathbf{S}(f, t) \sim \mathcal{CN}(\mathbf{H}(f) \mathbf{S}(f, t), \delta^{-1}(f)) \\ \mathbf{X} | \mathbf{S} \sim \prod_{f=1}^F \prod_{t=1}^T p(X(f, t) | \mathbf{S}(f, t)). \end{cases} \quad (6)$$

The probabilistic graphical model is summarized in Fig. 1.

B. Task Description

In this work, we aim to jointly complete speech dereverberation and blind RIR identification by solving all hidden variables and parameters in Fig. 1 through VBI.

For speech dereverberation, we care about the anechoic spectrum, which is a hidden variable in our probabilistic graphical model. We aim to get its maximum a posteriori (MAP) estimation given the reverberant microphone recording, written as

$$\hat{\mathbf{S}} = \arg \max_{\mathbf{S}} p(\mathbf{S} | \mathbf{X}), \quad (7)$$

where the posterior distribution of anechoic source signal can be represented according to the Bayes rule as

$$p(\mathbf{S} | \mathbf{X}) = \frac{p(\mathbf{S})p(\mathbf{X} | \mathbf{S})}{\int p(\mathbf{S})p(\mathbf{X} | \mathbf{S})d\mathbf{S}}. \quad (8)$$

For blind RIR identification, we care about the CTF filter, which is a model parameter in our probabilistic graphical model. Defining the CTF filter for all frequency bands as $\mathbf{H} = [\mathbf{H}(1), \dots, \mathbf{H}(F)]$, we aim to get its maximum likelihood (ML) estimation, written as

$$\hat{\mathbf{H}} = \arg \max_{\mathbf{H}} p(\mathbf{S}, \mathbf{X}). \quad (9)$$

The CTF filter is a representation of RIR in the T-F domain. We transform the CTF filter into the RIR waveform through a pseudo measurement process, a process that will be elaborated upon later.

III. PROPOSED METHOD

In this work, we propose a novel framework named VINP for joint speech dereverberation and blind RIR identification. We propose using an arbitrary discriminative dereverberation

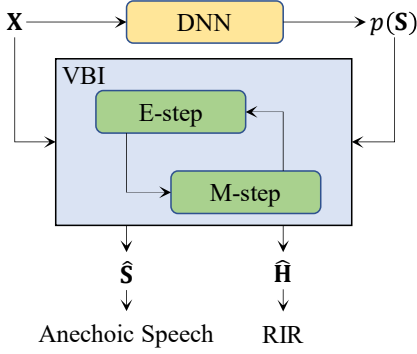


Fig. 2: Overview of VINP.

DNN to predict the prior distribution of anechoic speech from reverberant microphone recording and then applying VBI to analytically estimate the anechoic spectrum and the CTF filter. After that, we use a pseudo measurement process to transform the CTF filter into the RIR waveform. The overview of VINP is shown in Fig. 2.

A. Prediction of Anechoic Speech Prior

The direct-path speech signal, which is a scaled and delayed version of the anechoic source speech signal, is free from noise and reverberation as well. To avoid estimating the arbitrary direct-path propagation delay and attenuation, instead of the actual source speech, we setup the direct-path speech as the source speech and our target signal, still denoted as $s(n)$ or \mathbf{S} . Correspondingly, the RIR begins with the impulse response of the direct-path propagation.

In VINP, we consider the power spectrum of the direct-path speech signal as the variance of the anechoic speech prior $p(\mathbf{S})$. Then, in each T-F bin, the oracle estimation of precision $\alpha(f, t)$ is

$$\alpha(f, t) = 1/|S(f, t)|^2. \quad (10)$$

However, the oracle estimation is unavailable in practice. We propose integrating an arbitrary discriminative dereverberation DNN as an estimator of anechoic speech prior. Note that, in the proposed framework, we need to redesign the training loss function of the discriminative dereverberation DNNs.

Specifically, the discriminative DNN constructs a mapping from reverberant magnitude spectrum $|\mathbf{X}|$ to the anechoic magnitude spectrum $|\hat{\mathbf{S}}|$ as

$$|\hat{\mathbf{S}}| = f_{\text{DNN}}(|\mathbf{X}|). \quad (11)$$

Then Eq. (10) becomes

$$\alpha(f, t) = 1/|\hat{S}(f, t)|^2. \quad (12)$$

Regarding the loss function, we employ the average Kullback-Leibler (KL) divergence [39] to measure the distance

of estimated prior distribution $p(\hat{\mathbf{S}})$ and oracle prior distribution $p(\mathbf{S})$ as

$$\begin{aligned} \mathcal{L} &= \mathbb{E}_{\text{data}} \left[\frac{\text{KL} \left(p(\hat{\mathbf{S}}) || p(\mathbf{S}) \right)}{FT} \right] \\ &= \mathbb{E}_{\text{data}} \left[\frac{\sum_{f=1}^F \sum_{t=1}^T \left[\ln \left(\frac{|S(f, t)|^2}{|\hat{S}(f, t)|^2} \right) + \frac{|\hat{S}(f, t)|^2}{|S(f, t)|^2} - 1 \right]}{FT} \right]. \end{aligned} \quad (13)$$

In practice, we use

$$\begin{aligned} \mathcal{L} &= \mathbb{E}_{\text{data}} \left[\frac{\sum_{f=1}^F \sum_{t=1}^T \left[\ln \left(\frac{|S(f, t)|^2 + \epsilon}{|\hat{S}(f, t)|^2 + \epsilon} \right) + \frac{|\hat{S}(f, t)|^2 + \epsilon}{|S(f, t)|^2 + \epsilon} - 1 \right]}{FT} \right] \end{aligned} \quad (14)$$

instead to avoid numerical instabilities, where ϵ is a small constant. Such a loss function is different from that in regular discriminative dereverberation DNNs which directly predict the anechoic spectrum.

Research indicates that the complex nonlinear operations of DNNs often lead to outputs with unpredictable artificial errors. While these errors do not significantly affect speech perceptual quality, their impact on back-end speech recognition applications remains uncertain. As a result, DL-based approaches may not improve ASR performance [27], [40], [26]. However, in our method, by regarding the DNN output as a prior distribution of anechoic speech and utilizing the subsequent CTF-based VBI stage to refine it, this problem can be alleviated, leading to better ASR performance. Experiments in Section IV will provide evidence to support this conclusion.

B. Variational Bayesian Inference

Given the estimated prior distribution of anechoic speech and the observed recording, the estimation of every hidden variable and parameter is carried out through variational Bayesian inference.

The posterior distribution $p(\mathbf{S}|\mathbf{X})$ is intractable due to the integral term in Eq. (8). Therefore, we turn to VBI, which is a powerful tool for resolving hierarchical probabilistic models [11], [41]. More specifically, we employ the variational expectation-maximization (VEM) algorithm, which provides a way for approximating the complex posterior distribution $p(\mathbf{S}|\mathbf{X})$ with a factored distribution $q(\mathbf{S})$ according to the mean-field theory (MFT) as

$$p(\mathbf{S}|\mathbf{X}) \approx q(\mathbf{S}) = \prod_{f=1}^F \prod_{t=1}^T q(S(f, t)). \quad (15)$$

After factorization, VEM can estimate the posterior $q(\mathbf{S})$ and model parameters $\theta = \left\{ \delta(f) |_{f=1}^F, H(f, t) |_{f=1}^F, t=1}^T \right\}$ by E-step and M-step respectively and iteratively as

$$\ln q(S(f, t)) = \langle \ln p(\mathbf{S}, \mathbf{X}) \rangle_{\mathbf{S} \setminus S(f, t)} \quad (16)$$

and

$$\hat{\theta} = \arg \max_{\theta} \ln p(\mathbf{S}, \mathbf{X}), \quad (17)$$

where \setminus denotes the set subtraction and $\langle \cdot \rangle$ denotes expectation. Because the solution of such a probabilistic graphical model is an underdetermined problem, we do not update the precision parameter $\alpha(f, t)$ during the VEM iterations to prevent a deterioration in prior quality.

The specific update formulae are as follows:

1) *E-step*: In this step, we update the posterior distribution of the anechoic spectrum given the observation and estimated model parameters. Substitute the probabilistic model into Eq. (16), we have

$$\begin{aligned} \ln q(S(f, t)) &= \langle \ln p(\mathbf{S}, \mathbf{X}) \rangle_{\mathbf{S} \setminus S(f, t)} \\ &= \langle \ln p(S(f, t)) \rangle_{\mathbf{S} \setminus S(f, t)} \\ &\quad + \left\langle \sum_{l=0}^{L-1} \ln p(X(f, t+l) | \mathbf{S}(f, t+l)) \right\rangle_{\mathbf{S} \setminus S(f, t)} + c, \end{aligned} \quad (18)$$

where c is a constant term that is independent of $S(f, t)$, and

$$\begin{cases} \ln p(S(f, t)) = \ln \alpha(f, t) - \alpha(f, t) |S(f, t)|^2 + c \\ \ln p(X(f, t+l) | \mathbf{S}(f, t+l)) \\ = \ln \delta(f) - \delta(f) |X(f, t+l) - \mathbf{H}(f) \mathbf{S}(f, t+l)|^2 + c. \end{cases} \quad (19)$$

According to the property of Gaussian distribution, the posterior distribution is also Gaussian, written as

$$q(S(f, t)) = \mathcal{CN}(\mu(f, t), \gamma^{-1}(f, t)), \quad (20)$$

whose precision and mean have close-form solutions as

$$\begin{cases} \gamma(f, t) = \alpha(f, t) + \delta(f) \|\mathbf{H}(f)\|_2^2 \\ \mu(f, t) = \gamma^{-1}(f, t) \delta(f) \\ \times \left[\sum_{l=0}^{L-1} H_l(f)^* [X(f, t+l) - \mathbf{H}_{\setminus l}(f) \hat{\boldsymbol{\mu}}(f, t+l)] \right], \end{cases} \quad (21)$$

where $\mathbf{H}_{\setminus l}(f)$ is same as $\mathbf{H}(f)$ except that $H_l(f)$ is set to 0, and $\hat{\boldsymbol{\mu}}(f, t+l) = [\hat{\mu}(f, t+l-L+1), \dots, \hat{\mu}(f, t+l)]^T$ contains the estimates of means from the previous VEM iteration.

In order to make VEM converge more smoothly, we further apply an exponential moving average (EMA) to the estimates in Eq. (21) as

$$\begin{cases} \hat{\gamma}^{-1}(f, t) = \lambda \hat{\gamma}_{\text{pre}}^{-1}(f, t) + (1 - \lambda) \gamma^{-1}(f, t) \\ \hat{\mu}(f, t) = \lambda \hat{\mu}_{\text{pre}}(f, t) + (1 - \lambda) \mu(f, t), \end{cases} \quad (22)$$

where λ is a smoothing factor, $\hat{\mu}_{\text{pre}}(f, t)$ and $\hat{\gamma}_{\text{pre}}^{-1}(f, t)$ are the estimates from the previous VEM iteration.

The prior of anechoic speech narrows down the infinite number of possible solutions when decoupling the anechoic speech and the RIR, which is the key to achieving dereverberation [42]. The mean of the posterior distribution is the MAP estimate of anechoic spectrum $\hat{\mathbf{S}}$. It is also worth noticing that the E-step can be implemented in parallel across all T-F bins.

2) *M-step*: In this step, VEM updates the noise precision and CTF filter by maximizing the logarithmic joint probability of the anechoic speech and observation, which is

$$\begin{aligned} \ln p(\mathbf{S}, \mathbf{X}) &= \ln p(\mathbf{X} | \mathbf{S}) + c \\ &= T \ln \delta(f) - \delta(f) \sum_{t=1}^T |X(f, t) - \mathbf{H}(f) \mathbf{S}(f, t)|^2 + c, \end{aligned} \quad (23)$$

where c is a constant term that is independent of $\delta(f)$ and $\mathbf{H}(f)$. Setting the first derivative with respect to the parameters to zero, the noise precision is updated as

$$\begin{aligned} \hat{\delta}(f) &= T \left/ \sum_{t=1}^T \left[|X(f, t)|^2 - 2 \text{Re} \{ X^*(f, t) \mathbf{H}(f) \langle \mathbf{S}(f, t) \rangle \} \right. \right. \\ &\quad \left. \left. + \mathbf{H}(f) \langle \mathbf{S}(f, t) \mathbf{S}^H(f, t) \rangle \mathbf{H}^H(f) \right] \right., \end{aligned} \quad (24)$$

and the CTF filter is updated as

$$\begin{aligned} \hat{\mathbf{H}}(f) &= \left[\sum_{t=1}^T X(f, t) \langle \mathbf{S}^H(f, t) \rangle \right] \left[\sum_{t=1}^T \langle \mathbf{S}(f, t) \mathbf{S}^H(f, t) \rangle \right]^{-1}, \end{aligned} \quad (25)$$

where

$$\langle \mathbf{S}(f, t) \rangle = \boldsymbol{\mu}(f, t) = [\mu(f, t-L+1), \dots, \mu(f, t)]^T, \quad (26)$$

and

$$\begin{aligned} \langle \mathbf{S}(f, t) \mathbf{S}^H(f, t) \rangle &= \boldsymbol{\mu}(f, t) \boldsymbol{\mu}^H(f, t) \\ &\quad + \text{diag}([\alpha^{-1}(f, t-L+1), \dots, \alpha^{-1}(f, t)]), \end{aligned} \quad (27)$$

$\text{diag}(\cdot)$ denotes the operation of constructing a diagonal matrix. Just like the E-step, the M-step can also be implemented in parallel across all T-F bins.

3) *Initialization of VEM Parameters*: The initialization of parameters plays a crucial role in the convergence of VEM. Before iteration, the mean and variance of the anechoic speech posterior $p(\mathbf{S})$ are set to zero and the power spectrum of reverberant recording, respectively. This means we have

$$\begin{cases} \mu(f, t) = 0 \\ \alpha(f, t) = 1/|X(f, t)|^2. \end{cases} \quad (28)$$

The CTF coefficients in each frequency band are set to 0 except that the first coefficient is set to 1, which means

$$\begin{cases} H_0(f) = 1 \\ H_{l \neq 0}(f) = 0. \end{cases} \quad (29)$$

Because even during speech activity, the short-term power spectral density of observation often decays to values that are representative of the noise power level [43], the initial variance of the additional noise is set to the minimum power in each frequency band, which means

$$\delta(f) = \left[\min_t (|X(f, t)|^2) \right]^{-1}. \quad (30)$$

The VBI procedure is summarized in Algorithm 1. The final outputs of VBI procedure are the complex-valued anechoic spectrum and CTF filter estimates. Notice that in the proposed framework, the prior distribution of anechoic speech is not updated during iterations. Therefore, the DNN only infers once.

Algorithm 1 VBI procedure.

Input: Reverberant microphone recording \mathbf{X} ;

Output: Anechoic speech spectrum estimate $\hat{\mathbf{S}}$, CTF filter estimate $\hat{\mathbf{H}}$;

- 1: Estimate prior distribution of anechoic speech using Eq. (11) and Eq. (12);
 - 2: Initialize VEM parameters using Eq. (28), Eq. (29) and Eq. (30);
 - 3: **repeat**
 - 4: E-step: update the posterior distribution of anechoic speech using Eq. (21) and Eq. (22);
 - 5: M-step: update the parameter estimates of the signal model using Eq. (24) and Eq. (25);
 - 6: **until** Converge or reach the maximum number of iterations.
-

C. Transformation to Waveforms

After the VBI procedure, both the anechoic spectrum and the CTF filter are estimated. We need to further transform these T-F representations into waveforms. By applying inverse STFT to the anechoic spectrum estimate, we can easily get the anechoic speech waveform. For the estimation of RIR, we design a pseudo intrusive measurement process as follows.

A common method for intrusive measuring the RIR of an acoustical system is to apply a known excitation signal and measure the microphone recording [44]. Playing an excitation signal $e(n)$ with a loudspeaker, the noiseless microphone recording $y(n)$ can be written as

$$y(n) = h(n) * e(n), \quad (31)$$

where $h(n)$ has the same meaning as in Eq. (1). A commonly used logarithmic sine sweep excitation signal can be expressed as [44], [45]

$$e(n) = \sin \left[\frac{N\omega_1}{\ln(\omega_2/\omega_1)} \left(e^{n \ln(\omega_2/\omega_1)/N} - 1 \right) \right], \quad (32)$$

where ω_1 is the initial radian frequency and ω_2 is the final radian frequency of the sweep with duration N . Through an ideal inverse filter $v(n)$, the excitation signal can be transformed into a Dirac's delta function $\delta(n)$, as

$$e(n) * v(n) = \delta(n). \quad (33)$$

For the logarithmic sine sweep excitation, the inverse filter $v(n)$ is an amplitude-modulated and time-reversed version of itself [44], [45]. The RIR can be estimated by convolving the measurement $y(n)$ with the inverse filter $v(n)$ as

$$h(n) = y(n) * v(n). \quad (34)$$

In our approach, the excitation signal is convoluted by the CTF estimates (along the time dimension) to get a pseudo measurement $\tilde{Y}(f, t)$ in the T-F domain as

$$\tilde{Y}(f, t) = \hat{\mathbf{H}}(f) \mathbf{E}(f, t), \quad (35)$$

where $\mathbf{E}(f, t) = [E(f, t - L + 1), \dots, E(f, t)]^T \in \mathbb{C}^{L \times 1}$, $\tilde{Y}(f, t)$ and $E(f, t)$ are the STFT coefficient of $\tilde{y}(n)$ and $e(n)$, respectively. Finally, after applying inverse STFT to $\tilde{Y}(f, t)$, we use the pseudo measurement $\tilde{y}(n)$ to estimate the RIR waveform by

$$\hat{h}(n) = \tilde{y}(n) * v(n). \quad (36)$$

The transformation from the CTF filter to RIR waveform is summarized in Algorithm 2.

Algorithm 2 Transformation from CTF to RIR.

Input: CTF filter estimate $\hat{\mathbf{H}}$;

Output: RIR waveform estimate $\hat{h}(n)$;

- 1: Pick a pair of excitation signal $e(n)$ and its inverse filter $v(n)$;
 - 2: Build a pseudo measurement signal $\tilde{y}(n)$ using Eq. (35);
 - 3: Estimate RIR $\hat{h}(n)$ by inverse filtering as Eq. (36).
-

IV. EXPERIMENTS

A. Datasets

VINP is designed for both speech dereverberation and blind RIR identification. These two tasks share the same DNN for speech prior distribution prediction. Therefore, we use a single training set and two different test sets.

1) *Training Set:* The training set is composed of 200 hours of high-quality English speech utterances from the corpora of EARS [46], DNS Challenge [47], and VCTK [48]. All speech utterances are downsampled to 16 kHz if necessary. We simulate 100,000 pairs of reverberant and direct-path RIRs using the `gpuRIR` toolbox [49]. The simulated speaker and microphone are randomly placed in rooms with dimensions randomly selected within a range of 3 m to 15 m (for length and width) and 2.5 m to 6 m (for height). The minimum distance between the speaker/microphone and the wall is 1 m. Reverberant RIRs have RT60 values uniformly selected within the range of 0.2 s to 1.5 s. Direct-path RIRs are generated using the same geometric parameters as the reverberant ones but with an absorption coefficient of 0.99. Noise recordings from the Noise92 corpus and the training set from the REVERB Challenge [50] are employed. The signal-to-noise ratio (SNR) is randomly selected within the range of 5 dB to 20 dB.

2) *Test Set for Speech Dereverberation:* For speech dereverberation, we utilize the official single-channel test set from the REVERB Challenge [50], which includes both simulated data (marked as 'SimData') and real recordings (marked as 'RealData').

In SimData, there exist six distinct reverberation conditions: three room volumes (small, medium, and large), and two distances between the speaker and the microphone (50 cm and 200 cm). The RT60 values are approximately 0.25 s, 0.5 s, and 0.7 s. The noise is stationary background noise, mainly

generated by air conditioning systems. SimData has a SNR of 20 dB.

RealData consists of utterances spoken by human speakers in a noisy and reverberant meeting room. It includes two reverberation conditions: one room and two distances between the speaker and the microphone array (approximately 100 cm and 250 cm). The RT60 is about 0.7 s.

3) *Test Set for Blind RIR Identification*: A test set named 'SimACE' is constructed to evaluate blind RIR estimation. In SimACE, microphone signals are simulated by convolving the clean speech from the 'si_et_05' subset in WSJ0 corpus [51] with the downsampled recorded RIRs from the 'Single' subset in ACE Challenge [52], and adding noise from the test set in REVERB Challenge [50]. The minimum and maximum RT60s are 0.332 s and 1.22 s, respectively. More details about the RIRs can be found in [52]. We create the SimACE test set because the RT60 labels of the RIRs in SimACE are more accurate than those in REVERB Challenge. SimACE has a SNR of 20 dB.

B. Implementation of VINP

1) *Data Representation*: Before feeding the speech into VINP, the reverberant waveform is normalized by its maximum absolute value. Subsequently, the utterance is transformed using STFT with a Hann window of 512 samples (32 ms) and a hop length of 128 samples (8 ms).

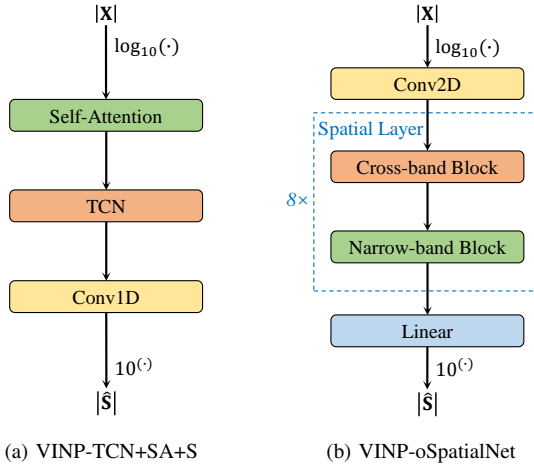


Fig. 3: DNN architectures in VINP.

2) *DNN Architecture*: VINP is able to employ any discriminative dereverberation DNNs to predict the prior distribution of anechoic speech. In this paper, we evaluate with the network proposed in TCN+SA+S [15] and a modified network of the Mamba version of oSpatialNet [53], resulting in two different versions marked as 'VINP-TCN+SA+S' and 'VINP-oSpatialNet', respectively. For both versions, the input and output of DNNs are the 10-based logarithmic magnitude spectra. To avoid numerical issues, a small constant 10^{-8} is added to the magnitude spectra before taking the logarithm.

The DNN architecture in VINP-TCN+SA+S is composed of temporal convolutional networks (TCNs) and self-attention

layers, as shown in Fig. 3. We use the same settings as the original TCN+SA+S [15], except that there is no activation function after the output layer and we do not use dropout.

The DNN architecture in VINP-oSpatialNet is derived from oSpatialNet [53], as depicted in Fig. 3. A two-dimensional convolution layer with a kernel size of 3×3 is employed to expand the input to 96 dimensions. The remaining modules are the same as those in the original oSpatialNet. Except that, for offline processing, we replace the second forward Mamba layer in the narrow-band block with a backward Mamba layer by simply reversing the input and output along the time dimension.

3) *Training Configuration*: For DNN training, we set the hyperparameter in the loss function to $\epsilon = 0.0001$. The speech utterances are segmented into 3 s. The batch size of VINP+TCN+SA+S and VINP-oSpatialNet are set to 16 and 4, respectively. The AdamW optimizer [54] with an initial learning rate of 0.001 is employed. The learning rate exponentially decays with $\text{lr} \leftarrow 0.001 \times 0.97^{\text{epoch}}$ and $\text{lr} \leftarrow 0.001 \times 0.9^{\text{epoch}}$ in VINP-TCN+SA+S and VINP-oSpatialNet, respectively. Gradient clipping is applied with a L2-norm threshold of 10. The training is carried out for 800,000 steps in total. We average the model weights of the best three epochs as the final model.

4) *VBI Settings*: The length of the CTF filter is set to $L = 30$. The fixed smoothing factor λ in Eq. (22) is set to 0.7 to obtain a stable result. In rare cases, if the likelihood of the complete data decreases, the VBI iteration will be stopped prematurely. Since the fundamental frequency of human speech is always higher than 85 Hz [55], we ignore the three lowest frequency bands and set their coefficients to zero to avoid the effect of extremely low SNR in these bands. Therefore, VBI processes a total of 254 frequency bands.

5) *Pseudo Excitation Signal*: We use a logarithmic sine sweep signal with a frequency range of 100 Hz to 8000 Hz and a duration of 5 s as the pseudo excitation signal. The formulae for the excitation signal and the corresponding inverse filter can be found in Eq. (32) and [44], [45].

6) *RT60 and DRR Estimation*: RT60 and DRR are key acoustic parameters that feature the characteristic of RIR, which are thus used in this work for evaluating the accuracy of RIR identification. RT60 and DRR can be directly calculated from RIR.

RT60 is the time required for the sound energy in an enclosure to decay by 60 dB after the sound source stops. Given the RIR waveform, Schroeder's integrated energy decay curve (EDC) is calculated as [56]

$$\text{EDC}(n) = \sum_{m=n}^{\infty} h^2(m). \quad (37)$$

Since the fact that sound energy decays exponentially over time, a linear fitting is applied to a portion of logarithmic EDC, and the slope is utilized to calculate RT60. During this process, the key to linear fitting lies in the heuristic strategy of selecting the fitting range. In this work, the starting point of linear fitting is selected within the range of a time delay from 20 ms to 50 ms at the direct-path sample, which represents the sample corresponding to the maximum value of the RIR. Meanwhile,

the ending point is established at a 5 dB attenuation relative to the starting point. We fit all intervals that meet the conditions and apply the result with the maximum absolute Pearson correlation coefficient to the estimation process of RT60 as

$$T_{60} = -60/k, \quad (38)$$

where k is the slope of the fitted line.

DRR refers to the ratio between the energy of the direct-path sound and the reverberant sound. In this work, the DRR is defined as

$$\text{DRR} = 10 \log_{10} \frac{\sum_{n=n_d-\Delta n_d}^{n_d+\Delta n_d} h^2(n)}{\sum_{n=0}^{n_d-\Delta n_d} h^2(n) + \sum_{n=n_d+\Delta n_d}^{\infty} h^2(n)}, \quad (39)$$

where the direct-path signal arrives at the n_d th sample, and Δn_d is the additional sample spread for the direct-path response which typically corresponds to 2.5 ms [52].

C. Comparison Methods

1) *Speech Dereverberation*: We compare VINP with various advanced dereverberation approaches including GWPE [4], SkipConvNet [57]², CMGAN [23]³, and StoRM [25]⁴. In addition, to demonstrate the effect of VINP, the DNNs in VINP-TCN+SA+S and VINP-oSpatialNet are also compared, i.e. TCN+SA+S [15] and oSpatialNet [53]. In TCN+SA+S, we use the recommended Griffin-Lim’s iterative algorithm [58] to restore the phase spectrum. In oSpatialNet, for a fair comparison, the backward Mamba is also applied to oSpatialNet. Different from VINP-oSpatialNet, the oSpatialNet employed for comparison processes the complex-valued speech spectrum as the original paper [53]. And this version is marked as ‘oSpatialNet*’.

For all comparison methods, we use their recommended configuration and official codes (if available). All DL-based approaches are trained from scratch on the same training set. GWPE is implemented using the NaraWPE python package [59]⁵.

The number of parameters and the multiply-accumulate operations per second (MACs, G/s) of the DL-based approaches are shown in Table I. Additionally, under the same settings of STFT and CTF length, a comparison of MACs per second and per iteration between the VEM algorithm in VINP and the EM algorithm in our previous work RVAE-EM [32] with regard to speech length is presented in Fig. 4. The asymptotic complexity of the VBI procedure in VINP is $O(FTL^2)$, indicating a linear growth with respect to the speech length, and its MACs is approximately a constant value of 0.27 G/s. In contrast, the asymptotic complexity of the EM algorithm in RVAE-EM is $O(FT^3)$ and there is always $T \gg L$.

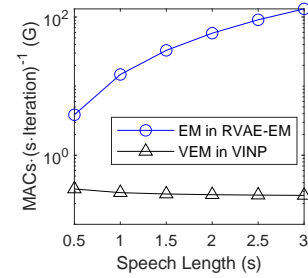


Fig. 4: MACs per second and per iteration versus speech length.

TABLE I: Number of parameters and MACs per second for DL-based methods

Method	Params (M)	MACs (G/s)
SkipConvNet [57]	64.3	11
CMGAN [23]	1.8	31
StoRM [25]	27.3+27.8=55.1	2300
TCN+SA+S [15]	4.7	0.7
oSpatialNet* [53]	1.7	36.6
VINP-TCN+SA+S	4.7	0.7+0.27×iterations
VINP-oSpatialNet	1.7	36.6+0.27×iterations

2) *Blind RIR Identification*: We measure RT60 and DRR through the RIR estimates to show the effectiveness of RIR identification. The comparison methods include several classical blind RT60 and DRR estimation methods, such as Ratnam’s approach [60]⁶ and Jeub’s approach [61]⁷. As a DL-based blind RIR identification method, BUDDy [35]⁸ is also compared. All these methods are implemented through the open-sourced official codes. Specifically, because the output of BUDDy is the RIR waveform, we employ the same implementation as in VINP to estimate the RT60 and DRR. Notice that the acoustic conditions of our training set and test set are mismatched. BUDDy, as an unsupervised approach, is designed to bridge the performance gap between scenarios with matched and mismatched acoustic conditions. Therefore, we directly employ the model parameters provided by the authors without retraining.

D. Evaluation Metrics

1) *Speech Dereverberation*: Speech dereverberation performance is evaluated in terms of both perception quality and ASR accuracy. We use the commonly used speech quality metrics including perceptual evaluation of speech quality (PESQ) [62], extended short-time objective intelligibility (ESTOI) [63], and deep noise suppression mean opinion score (DNSMOS) [64], [65]. Speech utterances are normalized by their maximum absolute value before evaluation. Higher scores indicate better speech quality and intelligibility.

To demonstrate the effectiveness of our method on ASR systems, we utilize the pre-trained Whisper [66] ‘tiny’ model

²<https://github.com/zehuachenImperial/SkipConvNet>

³<https://github.com/ruihezhecao96/CMGAN>

⁴<https://github.com/sp-uhh/storm>

⁵https://github.com/fgnt/nara_wpe

⁶https://github.com/nuniz/blind_rt60

⁷<https://ww2.mathworks.cn/matlabcentral/fileexchange/32752-blind-direct-to-reverberant-energy-ratio-drr-estimation>

⁸<https://github.com/sp-uhh/buddy>

TABLE II: Dereverberation results on REVERB (1-ch)

Method	SimData							RealData				
	PESQ	ESTOI	DNSMOS		WER (%)			DNSMOS		WER (%)		
			P.835	P.808	tiny	small	medium	P.835	P.808	tiny	small	medium
Unprocessed	1.48	0.70	2.37	3.20	12.7	5.6	4.7	1.31	2.82	21.1	7.7	5.6
Oracle	-	-	3.76	3.90	7.4	4.5	4.1	-	-	-	-	-
GWPE [4]	1.57	0.72	2.41	3.22	11.9	5.4	4.7	1.43	2.83	17.7	7.0	5.5
SkipConvNet [57]	2.12	0.81	3.20	3.60	12.9	6.4	5.3	2.74	3.32	26.1	9.3	7.4
CMGAN [23]	2.85	0.90	3.82	3.81	9.2	5.1	4.5	3.86	4.00	12.5	5.8	5.2
StoRM [25]	2.34	0.86	3.73	3.96	11.4	6.0	5.1	3.72	4.01	16.8	9.9	9.7
TCN+SA+S [15]	2.59	0.86	3.50	3.73	11.8	6.5	5.0	3.37	3.73	23.0	12.9	6.7
oSpatialNet* [53]	2.87	0.92	3.54	3.88	8.7	4.8	4.3	3.39	3.86	10.3	5.3	4.5
VINP-TCN+SA+S (prop.)	2.51	0.87	3.47	3.88	8.8	5.1	4.4	3.17	3.77	11.5	6.2	5.1
VINP-oSpatialNet (prop.)	2.82	0.90	3.48	3.86	8.1	4.8	4.3	3.32	3.80	9.1	5.0	4.3

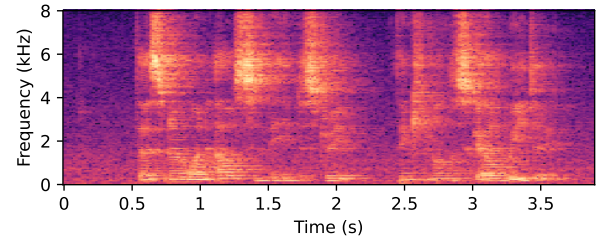
(with 39 M parameters), 'small' model (with 244 M parameters), and 'medium' model (with 769 M parameters) for ASR evaluation. No additional dataset-specific finetuning or retraining is applied before ASR inference. The word error rate (WER) is used as the evaluation metric. Lower WER indicates better ASR performance.

2) *Blind RIR Identification*: We use the accuracy of RT60 and DRR estimation to evaluate the performance of blind RIR identification. We present the mean absolute error (MAE) and the root mean square error (RMSE) of RT60 and DRR between their estimates and ground-truth values over the SimACE test set. Lower MAE and RMSE indicate better results.

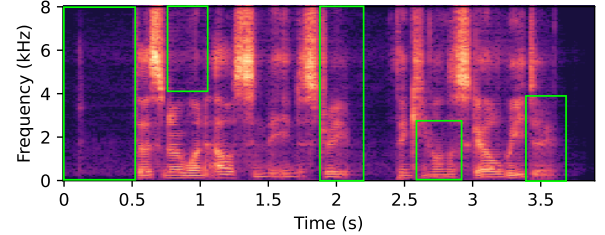
E. Results and Analysis

1) *Speech Dereverberation*: Setting the number of VEM iterations to 100, the dereverberation results are presented in Table II, where the bold font denotes the best two results.

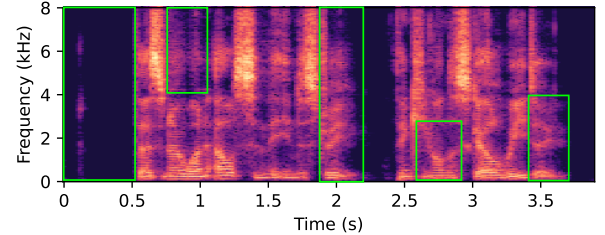
As the metrics of unprocessed speech and oracle speech indicate, a larger ASR system implies a stronger recognition ability for oracle speech and stronger robustness to reverberation. Compared with using a large ASR system alone, introducing an ASR-effective front-end speech dereverberation system can significantly improve the performance of ASR with fewer parameters and lower computational costs. Among the comparison methods, only a few approaches are proven to be effective for ASR, such as GWPE, CMGAN, oSpatialNet*, and the proposed VINP-TCN+SA+S and VINP-oSpatialNet. The classical GWPE yields a marginal improvement in ASR performance. Among the DL-based methods, SkipConvNet and TCN+SA+S encounter failures in ASR. Meanwhile, StoRM demonstrates effectiveness solely when the 'tiny' ASR model is employed. The reason for such ASR performance lies in the artifact induced by DNN, which is a common phenomenon in similar DL-based single-channel systems [26], [27]. Different from the comparison methods, VINP employs a linear CTF filtering process to model the reverberation effect and leverages the DNN output as a prior distribution of anechoic source speech. During the VBI procedure, VINP takes into account both this prior information and the observed data. By doing this, VINP circumvents the direct utilization of DNN output and thereby reduces the artifacts. Meanwhile, VINP still utilizes the powerful non-linear modeling ability of DNN.



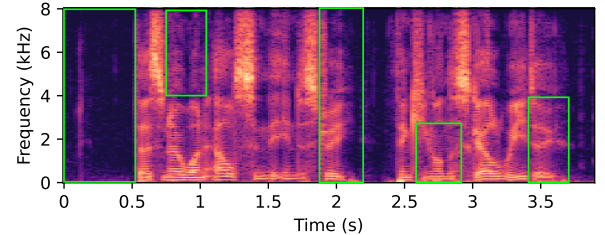
(a) Reverberant speech



(b) Output of TCN+SA+S



(c) Output of VINP-TCN+SA+S



(d) Oracle speech

Fig. 5: Examples of magnitude spectra (RT60=0.7 s).

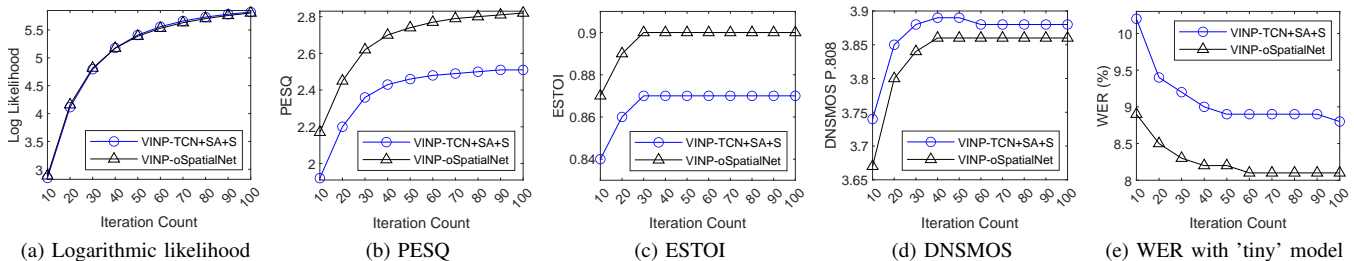


Fig. 6: Logarithmic likelihood and dereverberation metrics as a function of VEM iterations on REVERB SimData.

Consequently, VINP exhibits a remarkable superiority over the other approaches in ASR performance. When comparing VINP-TCN+SA+S with its backbone network TCN+SA+S, a gap in WER can be discerned, indicating that VINP can make an ASR-ineffective DNN effective. Both oSpatialNet* and VINP-oSpatialNet achieve ASR performance close to that of oracle speech on REVERB SimData when using the small and medium ASR systems. In other situations, a gap still exists, indicating that VINP can make an ASR-effective DNN even more effective. Because VINP-oSpatialNet provides an anechoic speech prior with higher quality, its ASR performance is superior to VINP-TCN+SA+S. Notably, VINP-oSpatialNet achieves SOTA performance in ASR.

Regarding speech quality, the ESTOI of VINP is roughly the same as that of the backbone network, while the PESQ shows a slight decrease compared to the backbone networks. This indicates that VINP is restricted by the capabilities of the backbone DNN. It is also worth noting that the PESQ increases with the growth of the number of VEM iterations, which we will demonstrate in detail in the experiments presented later. In subjective evaluation, the DNSMOS metrics of VINP-TCN+SA+S and VINP-oSpatialNet reach an advanced level. However, it does not rank the highest among all methods, especially when considering DNSMOS P.835. We hold the view that DNSMOS exhibits a certain preference for enhanced speech. As evidence, it can be seen that the DNSMOS of CMGAN and StoRM is even higher than that of oracle speech, indicating a preference for generative DNNs. In addition, VINP-TCN+SA+S and VINP-oSpatialNet exhibit worse and comparable performance to TCN+SA+S in DNSMOS P.835. However, in our auditory perception, the output speech of VINP exhibits a higher degree of naturalness. To illustrate the characteristics of different methods, examples of the reverberant speech, the output of TCN+SA+S, the output of VINP-TCN+SA+S, and the oracle speech are shown in Fig. 5. Due to the insufficient modeling capabilities of DNN, the output of TCN+SA+S has some overly smoothed artifacts. On the contrary, VINP-TCN+SA+S not only refers to the priors provided by DNNs, but also directly utilizes the observation during the VBI procedure, resulting in a better estimation of the anechoic speech spectrum. Moreover, VINP-TCN+SA+S demonstrates a better performance of background noise control. A series of enhanced audio examples are available online⁹.

TABLE III: Blind RT60 and DRR estimation results on SimACE

Method	RT60 (s)		DRR (dB)	
	MAE	RMSE	MAE	RMSE
Ratnam's [60]	0.151	0.182	-	-
Jaub's [61]	-	-	7.14	8.69
BUDDy [35]	0.089	0.132	3.93	4.57
VINP-TCN+SA+S (prop.)	0.079	0.094	3.83	4.27
VINP-oSpatialNet (prop.)	0.079	0.098	3.87	4.32

To illustrate the influence of VBI iterations on the performance of VINP, we show the average logarithmic likelihood of the complete data $\ln p(\mathbf{S}, \mathbf{X})$ (where the constant is omitted) and some metrics on REVERB SimData as the iteration count rises in Fig. 6. As the iteration count increases, the logarithmic likelihood and all metrics shift in a positive direction and tend to converge. Specifically, ESTOI, DNSMOS, and WER exhibit rapid convergence. In contrast, PESQ shows a continuous improvement that closely resembles the behavior of the logarithmic likelihood. This phenomenon indicates that better dereverberation performance can be achieved at the cost of computational complexity. Additionally, the capability of the backbone network determines the upper bound of performance of PESQ, ESTOI and DNSMOS. The logarithmic likelihood of VINP-TCN+SA+S and VINP-oSpatialNet converge to nearly the same values, yet their metrics are different, indicating that when the prior quality varies, the logarithmic likelihood cannot be directly used as an indicator to measure the enhancement performance.

2) *Blind RIR Identification*: Also setting the number of VEM iterations to 100, the RT60 and DRR estimation results are illustrated in Table III, where the bold font represents the best two results.

VINP surpasses all comparison methods, reaching the SOTA level for all metrics. Theoretically, one limitation of our method is that a CTF filter with a finite length can only model a RIR with a finite length. Nevertheless, it remains sufficient for RT60 and DRR estimation even under large-reverberation conditions, because the signal energy at the tail of the RIR is relatively negligible. From the perspective of spatial acoustic parameter estimation, VINP can estimate RIR well.

We also show the MAE of RT60 and DRR estimation as the iteration count rises in Fig. 7. As can be observed, as the iteration count increases, the errors of RT60 and DRR estimation decrease, which indicates an improved quality of

⁹<https://github.com/Audio-WestlakeU/VINP>

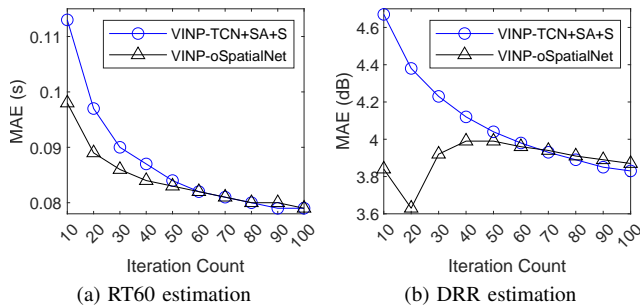


Fig. 7: MAE of RT60 and DRR estimation as a function of VEM iterations on SimACE.

RIR estimation. After 30 iterations, VINP-TCN+SA+S and VINP-oSpatialNet start to outperform BUDDy. When the iteration count is less than 70, VINP-oSpatialNet outperforms VINP-TCN+SA+S. Conversely, when the iteration count is larger than 70, VINP-TCN+SA+S is slightly superior to VINP-oSpatialNet. This phenomenon may be related to the DNN structure. Owing to the complexity of the entire system, we are currently unable to draw a conclusion about the preference for a specific DNN architecture for RIR identification. Unlike the experimental results of dereverberation, the identification of RIR does not seem to be sensitive to the capability of DNN when there are enough iterations.

V. CONCLUSION

In this paper, we propose a variational Bayesian inference framework with neural speech prior for joint ASR-effective speech dereverberation and blind RIR identification. By combining the prior distribution of anechoic speech predicted by an arbitrary discriminative dereverberation DNN with the reverberant recording, VINP employs VBI to solve the proposed CTF-based probabilistic graphical model and further estimate the anechoic speech and RIR. The usage of VBI avoids the direct utilization of DNN output but still utilizes its powerful nonlinear modeling capability, and proves to be effective for ASR without any joint training with the ASR system. Experimental results demonstrate that the proposed method achieves superior or competitive performance against the SOTA approaches in both tasks.

REFERENCES

- [1] T. Nakatani, T. Yoshioka, K. Kinoshita, M. Miyoshi, and B.-H. Juang, "Speech dereverberation based on variance-normalized delayed linear prediction," *IEEE Transactions on Audio, Speech, and Language Processing*, vol. 18, no. 7, pp. 1717–1731, 2010.
- [2] —, "Blind speech dereverberation with multi-channel linear prediction based on short time fourier transform representation," in *2008 IEEE International Conference on Acoustics, Speech and Signal Processing*, IEEE, 2008, pp. 85–88.
- [3] K. Kinoshita, M. Delcroix, T. Nakatani, and M. Miyoshi, "Suppression of late reverberation effect on speech signal using long-term multiple-step linear prediction," *IEEE transactions on audio, speech, and language processing*, vol. 17, no. 4, pp. 534–545, 2009.
- [4] T. Yoshioka and T. Nakatani, "Generalization of multi-channel linear prediction methods for blind mimo impulse response shortening," *IEEE Transactions on Audio, Speech, and Language Processing*, vol. 20, no. 10, pp. 2707–2720, 2012.

- [5] I. Kodrasi, T. Gerkmann, and S. Doclo, "Frequency-domain single-channel inverse filtering for speech dereverberation: Theory and practice," in *2014 IEEE International Conference on Acoustics, Speech and Signal Processing (ICASSP)*. IEEE, 2014, pp. 5177–5181.
- [6] D. Schmid, G. Enzner, S. Malik, D. Kolossa, and R. Martin, "Variational bayesian inference for multichannel dereverberation and noise reduction," *IEEE/ACM transactions on audio, speech, and language processing*, vol. 22, no. 8, pp. 1320–1335, 2014.
- [7] N. Mohammadiha and S. Doclo, "Speech dereverberation using non-negative convolutive transfer function and spectro-temporal modeling," *IEEE/ACM Transactions on Audio, Speech, and Language Processing*, vol. 24, no. 2, pp. 276–289, 2015.
- [8] Y. Laufer and S. Gannot, "A bayesian hierarchical model for speech enhancement," in *2018 IEEE International Conference on Acoustics, Speech and Signal Processing (ICASSP)*, 2018, pp. 46–50.
- [9] —, "A bayesian hierarchical model for speech enhancement with time-varying audio channel," *IEEE/ACM Transactions on Audio, Speech, and Language Processing*, vol. 27, no. 1, pp. 225–239, 2019.
- [10] Z. Yang, L. Xie, and C. Zhang, "Off-grid direction of arrival estimation using sparse bayesian inference," *IEEE transactions on signal processing*, vol. 61, no. 1, pp. 38–43, 2012.
- [11] P. Wang, H. Yang, and Z. Ye, "An off-grid wideband doa estimation method with the variational bayes expectation-maximization framework," *Signal Processing*, vol. 193, p. 108423, 2022.
- [12] P. Wang, F. Xiong, Z. Ye, and J. Feng, "Joint estimation of direction-of-arrival and distance for arrays with directional sensors based on sparse bayesian learning," in *INTERSPEECH*, 2022.
- [13] K. Han, Y. Wang, D. Wang, W. S. Woods, I. Merks, and T. Zhang, "Learning spectral mapping for speech dereverberation and denoising," *IEEE/ACM Transactions on Audio, Speech, and Language Processing*, vol. 23, no. 6, pp. 982–992, 2015.
- [14] Y. Luo and N. Mesgarani, "Real-time single-channel dereverberation and separation with time-domain audio separation network," in *Interspeech*, 2018, pp. 342–346.
- [15] Y. Zhao, D. Wang, B. Xu, and T. Zhang, "Monaural speech dereverberation using temporal convolutional networks with self attention," *IEEE/ACM transactions on audio, speech, and language processing*, vol. 28, pp. 1598–1607, 2020.
- [16] X. Hao, X. Su, R. Horaud, and X. Li, "Fullsubnet: A full-band and sub-band fusion model for real-time single-channel speech enhancement," in *ICASSP 2021-2021 IEEE International Conference on Acoustics, Speech and Signal Processing (ICASSP)*. IEEE, 2021, pp. 6633–6637.
- [17] R. Zhou, W. Zhu, and X. Li, "Speech dereverberation with a reverberation time shortening target," in *ICASSP 2023-2023 IEEE International Conference on Acoustics, Speech and Signal Processing (ICASSP)*. IEEE, 2023, pp. 1–5.
- [18] F. Xiong, W. Chen, P. Wang, X. Li, and J. Feng, "Spectro-temporal subnet for real-time monaural speech denoising and dereverberation," in *Interspeech*, 2022, pp. 931–935.
- [19] D. P. Kingma and M. Welling, "Auto-encoding variational bayes," in *ICLR*, 2014.
- [20] I. Goodfellow, J. Pouget-Abadie, M. Mirza, B. Xu, D. Warde-Farley, S. Ozair, A. Courville, and Y. Bengio, "Generative adversarial networks," *Communications of the ACM*, vol. 63, no. 11, pp. 139–144, 2020.
- [21] J. Ho, A. Jain, and P. Abbeel, "Denoising diffusion probabilistic models," *Advances in neural information processing systems*, vol. 33, pp. 6840–6851, 2020.
- [22] S.-W. Fu, C.-F. Liao, Y. Tsao, and S.-D. Lin, "Metricgan: Generative adversarial networks based black-box metric scores optimization for speech enhancement," in *International Conference on Machine Learning*. PmlR, 2019, pp. 2031–2041.
- [23] S. Abdulatif, R. Cao, and B. Yang, "Cmgan: Conformer-based metricgan for monaural speech enhancement," *IEEE/ACM Transactions on Audio, Speech, and Language Processing*, 2024.
- [24] J. Richter, S. Welker, J.-M. Lemerrier, B. Lay, and T. Gerkmann, "Speech enhancement and dereverberation with diffusion-based generative models," *IEEE/ACM Transactions on Audio, Speech, and Language Processing*, vol. 31, pp. 2351–2364, 2023.
- [25] J.-M. Lemerrier, J. Richter, S. Welker, and T. Gerkmann, "Storm: A diffusion-based stochastic regeneration model for speech enhancement and dereverberation," *IEEE/ACM Transactions on Audio, Speech, and Language Processing*, 2023.
- [26] K. Iwamoto, T. Ochiai, M. Delcroix, R. Ikeshita, H. Sato, S. Araki, and S. Katagiri, "How bad are artifacts?: Analyzing the impact of speech enhancement errors on asr," in *Interspeech 2022*, 2022, pp. 5418–5422.

- [27] —, “How does end-to-end speech recognition training impact speech enhancement artifacts?” in *ICASSP 2024-2024 IEEE International Conference on Acoustics, Speech and Signal Processing (ICASSP)*. IEEE, 2024, pp. 11 031–11 035.
- [28] G. J. Mysore and P. Smaragdis, “A non-negative approach to semi-supervised separation of speech from noise with the use of temporal dynamics,” in *2011 IEEE International Conference on Acoustics, Speech and Signal Processing (ICASSP)*. IEEE, 2011, pp. 17–20.
- [29] Y. Bando, M. Mimura, K. Itoyama, K. Yoshii, and T. Kawahara, “Statistical speech enhancement based on probabilistic integration of variational autoencoder and non-negative matrix factorization,” in *2018 IEEE International Conference on Acoustics, Speech and Signal Processing (ICASSP)*. IEEE, 2018, pp. 716–720.
- [30] X. Bie, S. Leglaive, X. Alameda-Pineda, and L. Girin, “Unsupervised speech enhancement using dynamical variational autoencoders,” *IEEE/ACM Transactions on Audio, Speech, and Language Processing*, vol. 30, pp. 2993–3007, 2022.
- [31] D. Baby and H. Bourlard, “Speech dereverberation using variational autoencoders,” in *ICASSP 2021-2021 IEEE International Conference on Acoustics, Speech and Signal Processing (ICASSP)*. IEEE, 2021, pp. 5784–5788.
- [32] P. Wang and X. Li, “Rvae-em: Generative speech dereverberation based on recurrent variational auto-encoder and convolutive transfer function,” in *ICASSP 2024-2024 IEEE International Conference on Acoustics, Speech and Signal Processing (ICASSP)*. IEEE, 2024, pp. 496–500.
- [33] C. J. Steinmetz, V. K. Ithapu, and P. Calamia, “Filtered noise shaping for time domain room impulse response estimation from reverberant speech,” in *2021 IEEE Workshop on Applications of Signal Processing to Audio and Acoustics (WASPAA)*. IEEE, 2021, pp. 221–225.
- [34] A. Richard, P. Dodds, and V. K. Ithapu, “Deep impulse responses: Estimating and parameterizing filters with deep networks,” in *ICASSP 2022-2022 IEEE International Conference on Acoustics, Speech and Signal Processing (ICASSP)*. IEEE, 2022, pp. 3209–3213.
- [35] J.-M. Lemerrier, E. Moliner, S. Welker, V. Välimäki, and T. Gerkmann, “Unsupervised blind joint dereverberation and room acoustics estimation with diffusion models,” *arXiv preprint arXiv:2408.07472*, 2024.
- [36] R. Talmon, I. Cohen, and S. Gannot, “Relative transfer function identification using convolutive transfer function approximation,” *IEEE Transactions on audio, speech, and language processing*, vol. 17, no. 4, pp. 546–555, 2009.
- [37] M. J. Beal, *Variational algorithms for approximate Bayesian inference*. University of London, University College London (United Kingdom), 2003.
- [38] D. G. Tzikas, A. C. Likas, and N. P. Galatsanos, “The variational approximation for bayesian inference,” *IEEE Signal Processing Magazine*, vol. 25, no. 6, pp. 131–146, 2008.
- [39] S. Kullback and R. A. Leibler, “On information and sufficiency,” *The annals of mathematical statistics*, vol. 22, no. 1, pp. 79–86, 1951.
- [40] T. Menne, R. Schlüter, and H. Ney, “Investigation into joint optimization of single channel speech enhancement and acoustic modeling for robust asr,” in *ICASSP 2019-2019 IEEE International Conference on Acoustics, Speech and Signal Processing (ICASSP)*. IEEE, 2019, pp. 6660–6664.
- [41] M. J. Bianco, P. Gerstoft, J. Traer, E. Ozanich, M. A. Roch, S. Gannot, and C.-A. Deledalle, “Machine learning in acoustics: Theory and applications,” *The Journal of the Acoustical Society of America*, vol. 146, no. 5, pp. 3590–3628, 2019.
- [42] Z.-Q. Wang, “Usdnet: Unsupervised speech dereverberation via neural forward filtering,” *IEEE/ACM Transactions on Audio, Speech, and Language Processing*, vol. 32, pp. 3882–3895, 2024.
- [43] R. Martin, “Noise power spectral density estimation based on optimal smoothing and minimum statistics,” *IEEE Transactions on speech and audio processing*, vol. 9, no. 5, pp. 504–512, 2001.
- [44] G.-B. Stan, J.-J. Embrechts, and D. Archambeau, “Comparison of different impulse response measurement techniques,” *Journal of the Audio engineering society*, vol. 50, no. 4, pp. 249–262, 2002.
- [45] A. Farina, “Simultaneous measurement of impulse response and distortion with a swept-sine technique,” in *Audio engineering society convention 108*. Audio Engineering Society, 2000.
- [46] J. Richter, Y.-C. Wu, S. Krenn, S. Welker, B. Lay, S. Watanabe, A. Richard, and T. Gerkmann, “EARS: An anechoic fullband speech dataset benchmarked for speech enhancement and dereverberation,” in *ISCA Interspeech*, 2024, pp. 4873–4877.
- [47] H. Dubey, A. Aazami, V. Gopal, B. Naderi, S. Braun, R. Cutler, H. Gamper, M. Golestaneh, and R. Aichner, “Icassp 2023 deep noise suppression challenge,” in *ICASSP*, 2023.
- [48] C. Valentini-Botinhao, X. Wang, S. Takaki, and J. Yamagishi, “Investigating rnn-based speech enhancement methods for noise-robust text-to-speech,” in *SSW*, 2016, pp. 146–152.
- [49] D. Diaz-Guerra, A. Miguel, and J. R. Beltran, “gpurr: A python library for room impulse response simulation with gpu acceleration,” *Multimedia Tools and Applications*, vol. 80, no. 4, pp. 5653–5671, 2021.
- [50] K. Kinoshita, M. Delcroix, T. Yoshioka, T. Nakatani, E. Habets, R. Haeb-Umbach, V. Leutnant, A. Sehr, W. Kellermann, R. Maas *et al.*, “The reverb challenge: A common evaluation framework for dereverberation and recognition of reverberant speech,” in *2013 IEEE Workshop on Applications of Signal Processing to Audio and Acoustics*. IEEE, 2013, pp. 1–4.
- [51] D. B. Paul and J. Baker, “The design for the wall street journal-based csr corpus,” in *Speech and Natural Language: Proceedings of a Workshop Held at Harriman, New York, February 23-26, 1992*, 1992.
- [52] J. Eaton, N. D. Gaubitch, A. H. Moore, and P. A. Naylor, “Estimation of room acoustic parameters: The ace challenge,” *IEEE/ACM Transactions on Audio, Speech, and Language Processing*, vol. 24, no. 10, pp. 1681–1693, 2016.
- [53] C. Quan and X. Li, “Multichannel long-term streaming neural speech enhancement for static and moving speakers,” *IEEE Signal Processing Letters*, vol. 31, pp. 2295–2299, 2024.
- [54] I. Loshchilov and F. Hutter, “Decoupled weight decay regularization,” in *ICLR*, 2018.
- [55] D. M. Howard and D. T. Murphy, *Voice science, acoustics, and recording*. Plural Publishing, 2007.
- [56] M. R. Schroeder, “New method of measuring reverberation time,” *The Journal of the Acoustical Society of America*, vol. 37, no. 6, Supplement, pp. 1187–1188, 1965.
- [57] V. Kothapally, W. Xia, S. Ghorbani, J. H. Hansen, W. Xue, and J. Huang, “Skipconvnet: Skip convolutional neural network for speech dereverberation using optimally smoothed spectral mapping,” *arXiv preprint arXiv:2007.09131*, 2020.
- [58] D. Griffin and J. Lim, “Signal estimation from modified short-time fourier transform,” *IEEE Transactions on acoustics, speech, and signal processing*, vol. 32, no. 2, pp. 236–243, 1984.
- [59] L. Drude, J. Heymann, C. Boeddeker, and R. Haeb-Umbach, “NARA-WPE: A python package for weighted prediction error dereverberation in Numpy and Tensorflow for online and offline processing,” in *13. ITG Fachtagung Sprachkommunikation (ITG 2018)*, Oct 2018.
- [60] R. Ratnam, D. L. Jones, B. C. Wheeler, W. D. O’Brien Jr, C. R. Lansing, and A. S. Feng, “Blind estimation of reverberation time,” *The Journal of the Acoustical Society of America*, vol. 114, no. 5, pp. 2877–2892, 2003.
- [61] M. Jeub, C. Nelke, C. Beaugeant, and P. Vary, “Blind estimation of the coherent-to-diffuse energy ratio from noisy speech signals,” in *2011 19th European Signal Processing Conference*. IEEE, 2011, pp. 1347–1351.
- [62] A. W. Rix, J. G. Beerends, M. P. Hollier, and A. P. Hekstra, “Perceptual evaluation of speech quality (pesq)-a new method for speech quality assessment of telephone networks and codecs,” in *2001 IEEE international conference on acoustics, speech, and signal processing. Proceedings (Cat. No. 01CH37221)*, vol. 2. IEEE, 2001, pp. 749–752.
- [63] J. Jensen and C. H. Taal, “An algorithm for predicting the intelligibility of speech masked by modulated noise maskers,” *IEEE/ACM Transactions on Audio, Speech, and Language Processing*, vol. 24, no. 11, pp. 2009–2022, 2016.
- [64] C. K. Reddy, V. Gopal, and R. Cutler, “Dnsmos: A non-intrusive perceptual objective speech quality metric to evaluate noise suppressors,” in *ICASSP 2021-2021 IEEE International Conference on Acoustics, Speech and Signal Processing (ICASSP)*. IEEE, 2021, pp. 6493–6497.
- [65] —, “Dnsmos p. 835: A non-intrusive perceptual objective speech quality metric to evaluate noise suppressors,” in *ICASSP 2022-2022 IEEE International Conference on Acoustics, Speech and Signal Processing (ICASSP)*. IEEE, 2022, pp. 886–890.
- [66] A. Radford, J. W. Kim, T. Xu, G. Brockman, C. McLeavey, and I. Sutskever, “Robust speech recognition via large-scale weak supervision,” in *International conference on machine learning*. PMLR, 2023, pp. 28 492–28 518.